Mucosal effects of tenofovir 1% gel

Florian Hladik[1,2,5*], Adam Burgener[8,9], Lamar Ballweber[5], Raphael Gottardo[4,5,6], Slim Fourati[7], James Y. Dai[4,6], Mark J. Cameron[7], Lucia Vojtech[1], Johanna Strobl[5], Sean M. Hughes[1], Craig Hoesley[10], Philip Andrew[12], Sherri Johnson[12], Jeanna Piper[13], David R. Friend[14], T. Blake Ball[8,9], Ross D. Cranston[11,16], Kenneth H. Mayer[15], M. Juliana McElrath[2,3,5] & Ian McGowan[11,16]

Departments of [1]Obstetrics and Gynecology, [2]Medicine, [3]Global Health, [4]Biostatistics, University of Washington, Seattle, USA; [5]Vaccine and Infectious Disease Division, [6]Public Health Sciences Division, Fred Hutchinson Cancer Research Center, Seattle, USA; [7]Vaccine and Gene Therapy Institute, Florida, Port St. Lucie, USA; [8]Department of Medical Microbiology, University of Manitoba, Winnipeg, Canada; [9]National HIV and Retrovirology Laboratories, Public Health Agency of Canada; [10]University of Alabama, Birmingham, USA; [11]University of Pittsburgh School of Medicine, Pittsburgh, USA; [12]FHI 360, Durham, USA; [13]Division of AIDS, NIAID, NIH, Bethesda, USA; [14]CONRAD, Eastern Virginia Medical School, Arlington, USA; [15]Fenway Health, Beth Israel Deaconess Hospital and Harvard Medical School, Boston, USA; [16]Microbicide Trials Network, Magee-Women's Research Institute, Pittsburgh, USA.

Abstract

BACKGROUND Tenofovir gel is being evaluated for vaginal and rectal pre-exposure prophylaxis against sexual HIV transmission. Because this is a new prevention strategy targeting large numbers of healthy people, we broadly assessed its effects on the mucosa.

METHODS AND FINDINGS In MTN-007, a phase 1, randomized, double-blinded rectal microbicide trial, we used systems genomics/proteomics to determine the effect of tenofovir 1% gel, nonoxynol-9 2% gel, placebo gel or no treatment on rectal biopsies taken at baseline, after one application or after seven daily applications (15 subjects/arm). Experiments were repeated using primary vaginal epithelial cells from four healthy women. After seven days of administration, tenofovir 1% gel had broad-ranging biological effects on the rectal mucosa, which were much more pronounced than—but different from—those caused by the detergent nonoxynol-9. Tenofovir profoundly suppressed anti-inflammatory mediators such as interleukin 10; increased T cell densities; caused mitochondrial dysfunction, possibly by blocking PNPT1 expression; and altered regulatory pathways of cell differentiation and survival. Except for leukocyte-derived factors, all these effects were replicated in primary vaginal epithelial cells, which also proliferated significantly faster in tenofovir's presence.

CONCLUSIONS Tenofovir's suppression of anti-inflammatory activity could diminish its prophylactic efficacy over time. The breadth of mucosal changes, including mitochondrial dysfunction and epithelial proliferation, raises questions about its safety for long-term topical use. These findings suggest that a systems biology evaluation of mucosal effects may be beneficial before advancing to large-scale efficacy trials with topical HIV prevention agents that achieve high, long-lasting local drug concentrations.

Introduction

The HIV prevention field has invested considerable resources in testing the phosphonated nucleoside reverse transcriptase inhibitor (NRTI) tenofovir as a mucosally-applied topical microbicide to prevent sexual HIV transmission. In a phase 2B trial, CAPRISA 004, pericoital tenofovir 1% gel was 39% efficacious in preventing vaginal HIV acquisition[1]. However, in another phase 2B trial, the VOICE study (MTN-003), the daily vaginal tenofovir 1% gel arm was discontinued for futility[2].

Adherence to product use was low in VOICE, likely explaining the differences in findings between the two studies. However, more frequent tenofovir gel exposure in VOICE (daily), as compared to pericoital use in CAPRISA 004, may also have contributed to this discrepancy.

A reduced glycerin formulation of the vaginal tenofovir 1% gel for use as a rectal microbicide appears safe when evaluated by epithelial sloughing, fecal calprotectin, inflammatory cytokine mRNA/protein levels and cellular immune activation markers[3]. However, because topical application of an antiretroviral drug to the mucosa is a novel prevention strategy without clinical precedent, we conducted a comprehensive systems biology assessment of tenofovir gel's effects on the mucosa.

Results

Tenofovir 1% gel induces broad and pronounced gene expression changes in the rectum

We measured mRNA expression changes across the complete human transcriptome by microarray (Illumina HumanHT12 v4 Expression BeadChips) in rectal biopsies taken at 9 and 15 cm proximal to the anal margin. Biopsies were obtained before treatment, after a single and after seven consecutive once-daily applications of reduced glycerin tenofovir 1% gel, nonoxynol-9 (N-9) 2% gel, hydroxyethyl cellulose (HEC) placebo gel, or no treatment (8 participants per arm were tested by microarrays). The primary results of the clinical study, MTN-007, a phase 1, randomized, double-blind, placebo-controlled trial at three US sites were reported elsewhere[3]. Relative to enrollment biopsies, after seven days of treatment, tenofovir 1% gel suppressed 505 genes and induced 137 genes in the 9 cm biopsies, whereas the detergent N-9, a transient mucosal toxin, suppressed 56 genes and induced 60 genes ($\log_2$ fold expression change ≥0.5 for induction or ≤-0.5 for suppression, FDR≤0.05) (Figure 1A,B). Fifteen suppressed and four induced genes were common to tenofovir and N-9 (Figure 1B). In the HEC gel and no treatment arms, 16 and 23 genes changed (Figure 1B). Tenofovir 1% gel affected more genes after seven days of treatment than after a single application and more genes in 9 cm than in 15 cm biopsies (Figure 1B), with significant correlations between expression changes at 9 cm and 15 cm (suppression: Spearman rho=0.4775; p<0.0001, Figure 1C; induction: Spearman rho=0.427; p<0.0001, Figure S1). Tenofovir suppressed genes more strongly than N-9 (median 0.505 vs 0.627 fold; p<0.0001), but induced genes less strongly (1.58 vs 1.69 fold; p=0.0002) (Figure S2).

Confirmatory RT-ddPCR quantification and in situ immunostaining in additional study participants

To independently confirm the microarray results, we selected nine induced and six suppressed genes and performed reverse transcription digital droplet PCR (RT-ddPCR) assays with RNA from the 9 cm biopsies in the remaining seven individuals enrolled in the tenofovir 1% gel arm (Figure 2). The mRNA copy numbers of all 15 genes increased or decreased as predicted from the microarray data between baseline and time point VII (Figure 2A,B). Next, we combined the microarray and RT-ddPCR expression data, normalized fluorescence and copy number values over their respective baselines, and compared the fold change after seven days of treatment with baseline (Figure 2C). Expression changes for all 15 genes assessed by microarray and RT-ddPCR were statistically significant (p<0.01 for all genes except TRIM5 [p=0.02]).

For additional confirmation, we selected three induced (CD7, CD3 and ubiquitin D) and one suppressed gene (IL-10) for immunohistochemical staining of the respective proteins in 9 cm rectal biopsies from 10 subjects (Figure 2D, Figure S3 and Figure S4). Consistent with the gene expression studies,

---

Figure 1. Tenofovir-induced gene expression changes in the human rectum

A Heat map of differentially expressed genes in 8 participants after a single (I) and after 7 consecutive once-daily (VII) rectal applications of tenofovir 1% gel compared to baseline in biopsies taken at 9 cm and 15 cm proximal to the anal margin. Red and green bars signify strength of gene induction and suppression, respectively. 642 genes are shown, all of which exhibited an estimated FDR≤0.05 and a log2 fold expression change of ≥0.5 (induction) or ≤-0.5 (suppression) when evaluated jointly for all 8 participants at time point VII in the 9 cm biopsies.

B Numbers of significantly suppressed (green borders and numbers) and induced (red borders and numbers) genes after reduced glycerin tenofovir 1% gel (TFV) treatment and their overlap with nonoxynol-9 (N-9), hydroxyethyl cellulose (HEC) and no treatment (No tx). Circle area symbolizes the number of affected genes, overlap the number of genes independently affected by two or three conditions.

C Correlation of log2 fold gene suppression from baseline to Day VII between 9 and 15 cm biopsies. All 505 genes significantly suppressed at 9 cm are included. Genes depicted as blue dots were significantly suppressed in both 9 and 15 cm biopsies (15 cm FDR<0.05), genes depicted as black dots were only significant in 9 cm biopsies (15 cm FDR≥0.05). Spearman rho correlation between the 9 and 15 cm biopsies expression and the corresponding p-value of a Spearman rank correlation test are indicated on the plot. Genes tested in Figure S2 and Figure S5 by RT-ddPCR are specifically indicated.

2
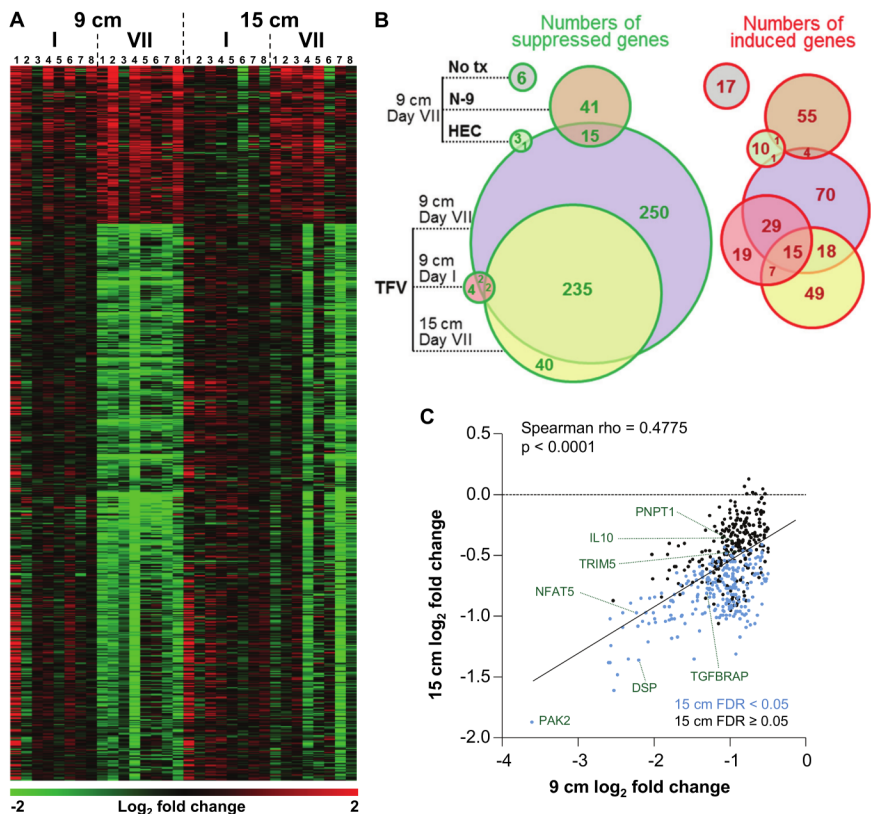
infiltrating T lymphocytes increased three- to six-fold in the mucosa (p=0.0006 for CD7+ and p=0.023 for CD3+), whereas IL-10+ columnar epithelial cells decreased by more than half (p=0.017), between baseline and following seven days of tenofovir 1% gel use. Ubiquitin D was widely expressed in all biopsies, but tenofovir treatment increased the intensity of its expression (p=0.007), as predicted by the microarrays.

Gene expression patterns and functional pathways

Tenofovir 1% gel was more suppressive than stimulatory, with a ratio of induced to suppressed genes in the 9 cm rectal biopsies of 0.116 (17 genes up-regulated to 146 down) for nuclear products. However, genes encoding secreted proteins were more often induced than suppressed (Figure 3A), with a ratio of 2.33 (35 genes up-regulated to 15 down; χ^2 p<0.0001). Noteworthy among induced genes for secreted products were

the chemokines CCL2, CCL19, CCL21, CCL23, CXCL9 and CXCL13 (Figure 3A). Correspondingly, transcripts of a number of leukocyte-specific cell surface markers increased, specifically CD2, CD3D, CD7, CD8A, CD19, CD52, CD53, CCR6 and CCR7. The kinetics of gene induction is depicted in Figure S5.

Among suppressed genes with products localizing to the cell nucleus, we identified a large number of known or putative transcription factors and their co-factors, including CREB1 (CAMP responsive element-binding protein 1) and CREBBP (CREB-binding protein), both activators of IL-10 transcription[26,27], NFAT5 (nuclear factor of activated T cells 5)[28], and many zinc finger proteins (Figure 3A). Tenofovir 1% gel also suppressed genes important for regulation of transcription and translation, as well as biological processes involving

Figure 2. Confirmation of microarray data

A,B Quantification of mRNA copy numbers measured in 9 cm biopsies by reverse transcription (RT) droplet digital PCR (ddPCR) relative to the housekeeping gene hemoglobin beta (HBB) copy numbers in seven additional study participants.

A Nine selected genes induced in the microarrays: CCL19, CCL21, CCL23, CXCL9, CCR7, CD7, CD19, matrix metallopeptidase 12 (MMP12) and serine protease inhibitor of the Kazal type 4 (SPINK4). Copy numbers at baseline (0), after a single tenofovir gel application (I) and after seven consecutive once-daily applications (VII) are shown. Line colors signify each of the seven study participants.

B Six selected suppressed genes: p21-activated kinase (PAK2), nuclear factor of activated T cells 5 (NFAT5), desmoplakin (DSP), TGF-β receptor associated protein (TGFBRAP), interleukin 10 (IL-10) and tripartite motif-containing protein 5 (TRIM5).

C Normalized fold changes of gene expression at Day VII over baseline in all 15 individuals treated with tenofovir 1% gel. Red dots depict fold changes measured by microarray, blue dots depict fold changes measured by RT-ddPCR. The boxes indicate median and 25th to 75th percentiles and the whiskers indicate 10th to 90th percentile. Asterisks indicate statistical significance level relative to baseline (one asterisk p<0.05; two asterisks p<0.01, by one-sided Wilcoxon tests, adjusted for multiple testing).

D Immunostaining of formalin-fixed 9 cm rectal biopsies from ten participants for the proteins CD7 (immunohistochemistry [IHC]), CD3 (immunofluorescence) and ubiquitin D (UBD; IHC), predicted to be induced by the microarrays, and for IL-10 (IHC), predicted to be suppressed. For CD7 and CD3, tissue sections were evaluated in their entirety and positive cells per mm² are shown at baseline (0) and after seven consecutive once-daily applications (VII). Representative images are shown in Figure S3. For UBD and IL-10, only columnar epithelial cells were evaluated. For UBD, the average mean staining intensities (MSI) per cell are shown. Representative images are shown in Figure S4.

Colors signify each of the ten study participants. The boxes indicate median and 25th to 75th percentiles and the whiskers indicate the range. Paired Wilcoxon signed-rank test p values for differences between 0 and VII are listed.
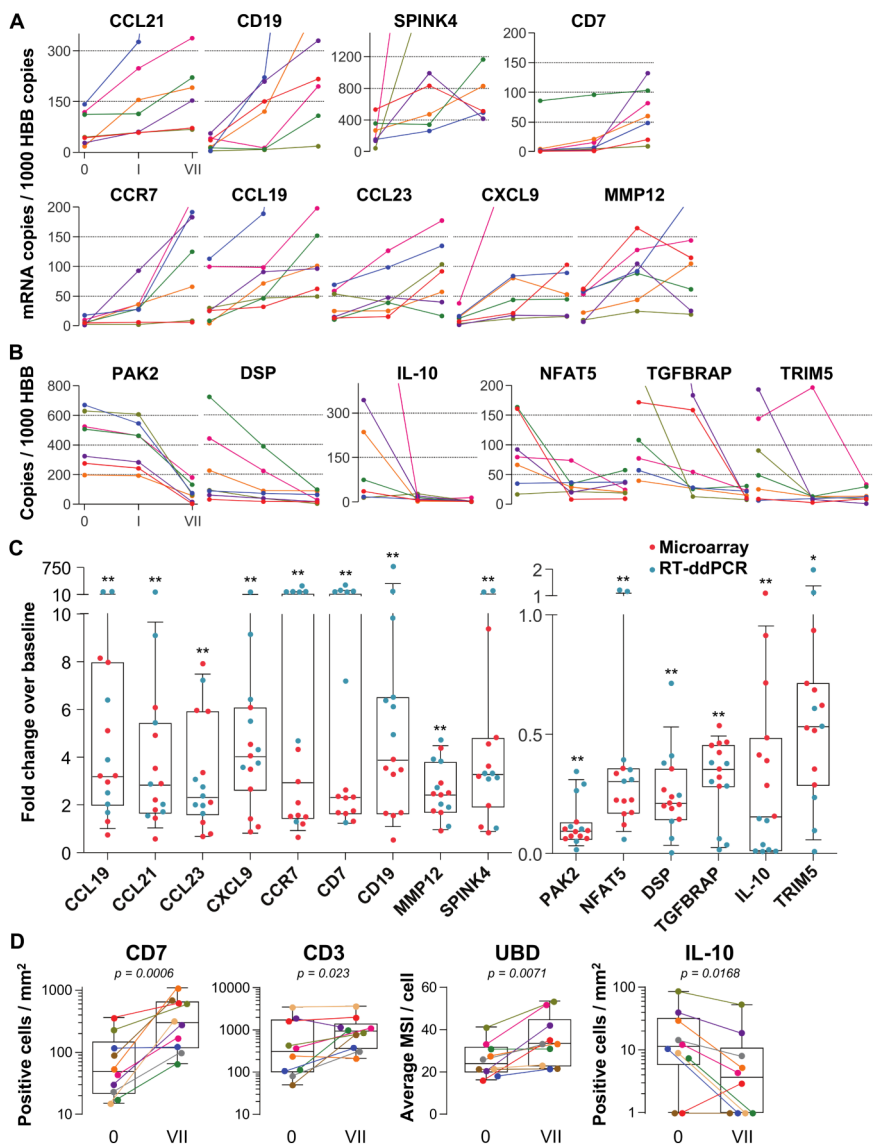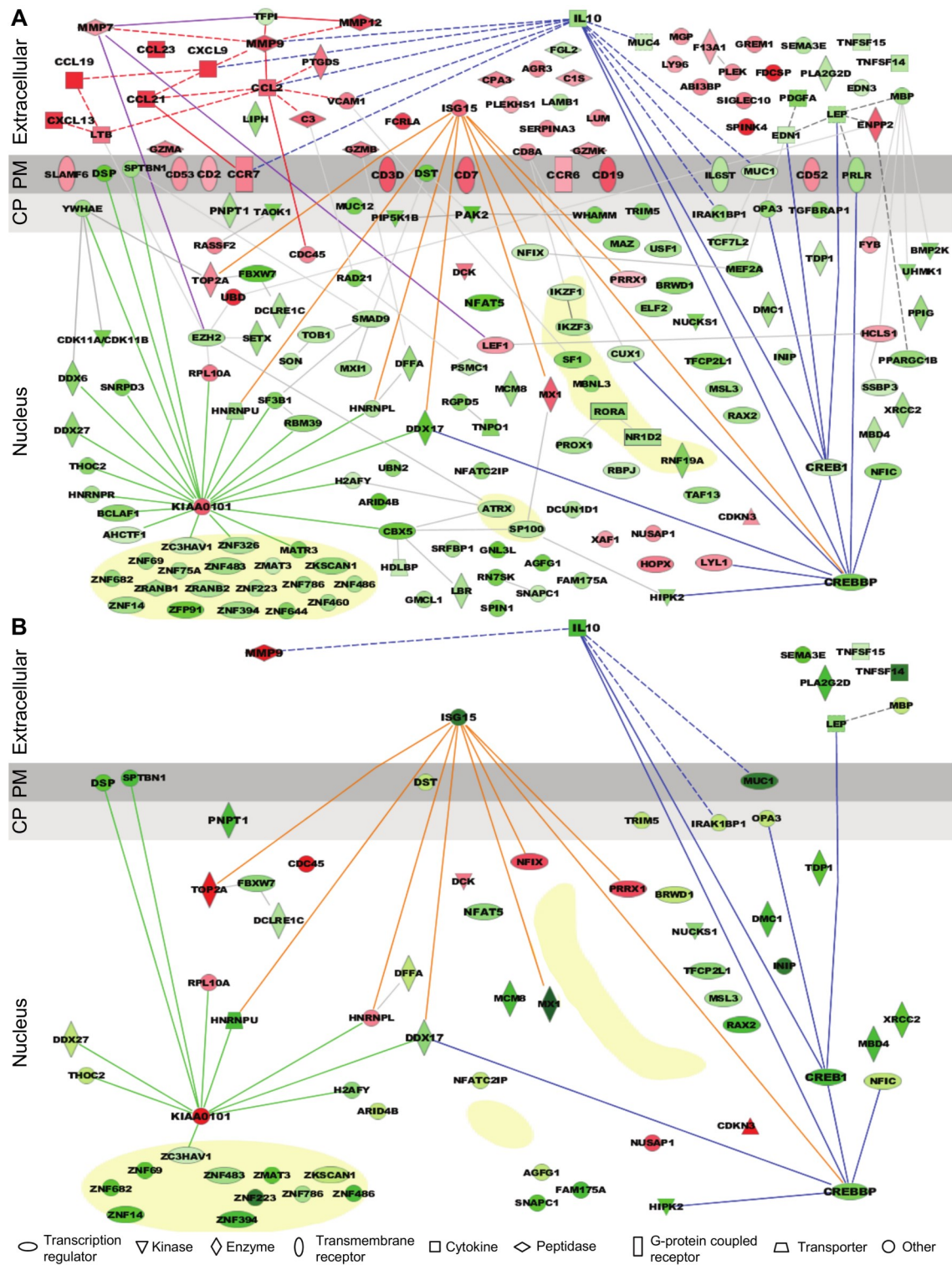
Figure 3. Expression pattern and functional pathway analysis

A Ingenuity pathways analysis of tenofovir-induced effects in rectal biopsies, showing cellular localizations of and relationships between individual gene products. Red symbols indicate induction and green symbols suppression at Day VII relative to baseline in 9 cm biopsies. The diagram includes all significant genes identified as primarily located in the extracellular space and the cell nucleus. A few selected significant genes with products localizing to the plasma membrane (PM) or cytoplasm (CP) are also shown based on their putative functional roles. Direct (solid lines) and indirect (dashed) interactions between gene products are indicated. Line color is arbitrary, and meant to

indicate relationships between groups of genes. Yellow shaded areas indicate zinc finger transcription factors.

B Pathways analysis of tenofovir-induced effects in primary vaginal epithelial cells. Only genes that were suppressed or induced by tenofovir both in 9 cm rectum in vivo and in vaginal epithelial cells in vitro are shown. Primary vaginal epithelial cells derived from three healthy women were cultured with 50 or 500 μM tenofovir for 14 days. Global gene expression microarrays at 4, 7 and 14 days of culture were evaluated in comparison to untreated epithelial cells. Pre-processed microarray expression data were extremely consistent between the three vaginal cell cultures (mean Pearson correlation coefficient 0.9912; Table S1).

transforming growth factor beta (TGFβ), epithelial structure organization, regulation of cell proliferation, and apoptosis (Figure S6). Lastly, tenofovir 1% gel suppressed genes important for mitochondrial function, including PNPT1 (polyribonucleotide nucleotidyltransferase 1)[29] and OPA3 (optic atrophy 3)[30]. Among the few genes with nuclear products that were strongly induced, KIAA0101 and ubiquitin D were notable[31-33].

Similarities between vaginal keratinocytes and rectal biopsies

Tenofovir 1% gel is most advanced as a candidate product for vaginal HIV prevention. We were therefore interested to extend our findings from the rectum to the vaginal mucosa. We isolated epithelial cells from vaginal tissues donated by three healthy women and tested their response to 50 and 500 µM tenofovir in vitro for up to 14 days of culture using RNA expression analysis. Preliminary tests showed that these dosages give roughly similar intracellular concentrations of the active drug (tenofovir diphosphate) as measured in the vagina after tenofovir 1% gel use (not shown)[7]. Tenofovir's effects on the purified vaginal epithelial cells (Figure 3B) were similar to its effects on the rectal mucosa (Figure 3A), but, as expected, changes likely driven by leukocytes in the biopsies were not seen in the purified epithelial cells, or were differently regulated. In the epithelial cells, tenofovir did not significantly change chemokine, chemokine receptor and cluster of differentiation (CD) genes, and it suppressed ISG 15 (interferon-stimulated gene 15) and MX1 (myxovirus resistance 1), which were induced in the biopsies.

The number of genes affected was initially higher with 500 µM than with 50 µM tenofovir, but equalized after 14 days of culture (Figure 4A). Next, we confirmed the expression changes of select genes by ddPCR with vaginal epithelial cells from four healthy women: mRNA copies of DSP (desmoplakin) and IL-10 significantly decreased, and KIAA0101 significantly increased during 7 days of tenofovir treatment, as seen in the microarray data (Figure 4B). In fact, IL-10 transcripts were virtually eliminated at 7 days (p<0.01), and KIAA0101 increased more than ten-fold at 500 µM tenofovir (p<0.01). By ELISA of cell lysates, IL-10 protein also decreased significantly (n=4 cell lines, p=0.0002) (Figure 4C).

Tenofovir treatment of primary vaginal epithelial cells in vitro mostly impacted the same biological processes as it did in the rectum in vivo (Figure 4D and Figure S6). Additionally, it suppressed genes important for keratinocyte differentiation and cellular innate immunity, and induced genes involved in DNA damage repair. Furthermore, tenofovir enhanced vaginal epithelial cell proliferation and/or cell survival in vitro (p=0.02) (Figure 4E).

Signs of mitochondrial toxicity

Our microarray results indicated that tenofovir suppresses PNPT1 (Figure 1C), which has been characterized as a master regulator of RNA import into mitochondria and whose deletion impairs mitochondrial function[29]. To explore tenofovir's effects on mitochondria, we first confirmed its inhibition of PNPT1 in the 9 cm and 15 cm rectal biopsies of all 15 study
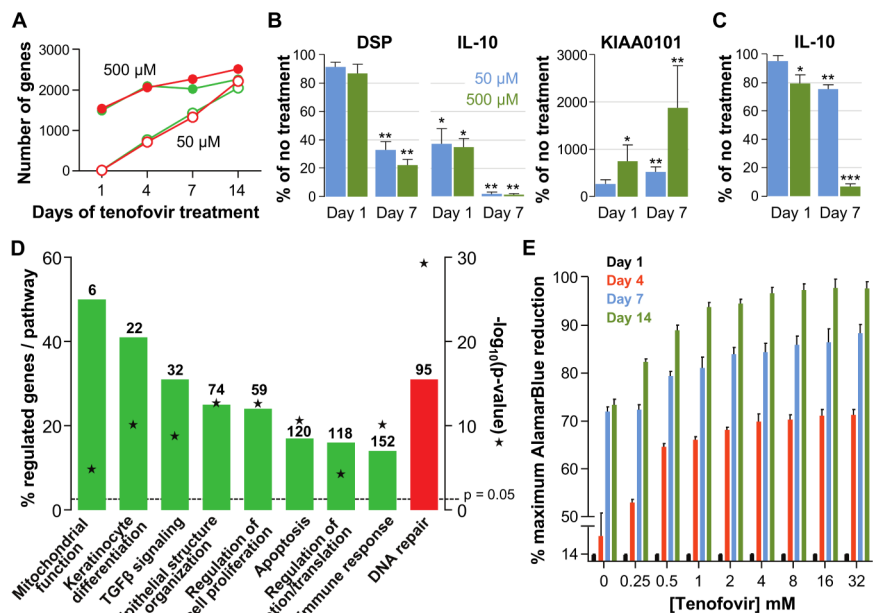
Figure 4. Effects of tenofovir on primary vaginal epithelial cells

A Number of suppressed (green) and induced (red) genes in response to treatment with 50 µM (open circles) or 500 µM (filled circles) tenofovir for 1, 4, 7 or 14 days (n=3 cell lines from different women).

B Quantification of mRNA copy numbers at days 1 and 7 of culture by RT-ddPCR assays for two selected genes identified as suppressed (DSP and IL-10) and one induced (KIAA0101) in the microarray data set (n=4 cell lines).

C Quantification of IL-10 protein concentrations in vaginal epithelial cells at days 1 and 7 of culture by ELISA. Mean (± standard deviation) IL-10 concentrations in the untreated cultures were 5.65 pg/ml (± 0.25) at day 1 and 5.86 pg/ml (± 0.32) at day 7 of culture. Boxes and error bars in (b) and (c) signify means and standard deviations with vaginal epithelial cell cultures derived from four healthy women. Asterisks indicate statistical significance level relative to untreated (*, p<0.05; **, p<0.01; ***, p<0.001).

D Selected biological processes defined in the InnateDB and DAVID databases with significant enrichment of genes suppressed or induced by 50 µM tenofovir in vaginal epithelial cells after 7 days of culture. Green bars depict the percentage of genes identified as suppressed in a particular process out of the total number of genes included in that process. Red bars depict gene induction. Numbers of suppressed and induced genes are indicated above the bars. Gene enrichment in each biological process was tested for statistical significance as described in the Methods and the computed p values are depicted by the stars. Not all processes with significant gene enrichment are

shown.

E Proliferation of vaginal epithelial cells without or with various concentrations of tenofovir (n =3 cell lines). Boxes depict mean percent reduction of the AlamarBlue reagent in comparison to the maximum reduction. Error bars signify standard deviations.

participants by RT-ddPCR. PNPT1 copy numbers decreased more than ten-fold at 9 cm (p<0.001) and by half at 15 cm (p<0.001) after 7 days of treatment (Figure 5A). To directly assess mitochondrial function, we picked one of the 13 genes encoded by mitochondrial DNA, ATP synthase F0 subunit 6 (ATP6), a key component of the proton channel[34], and measured its transcription by RT-ddPCR in the 9 cm biopsies of all 15 study participants in the tenofovir arm (Figure 5B). Because mitochondrial genes are not included on the microarray chips, we had no preexisting information on its expression. ATP6 mRNA copy numbers decreased on average three-fold (p<0.01) after a single application and six-fold after seven days (p<0.001). In contrast, ATP6 copy numbers were stable in all 15 study participants treated with 2% N-9 gel (p=0.4911) (Figure 5B).

Next, we evaluated changes in mitochondrial number and size between baseline and after seven days of treatment in two study participants chosen for exhibiting pronounced PNPT1 suppression by tenofovir. The number of mitochondria per μm^2 decreased by more than half after seven days of tenofovir treatment (p<0.001) (Figure 5C). In the second participant, mitochondria also increased in size by 1.4-fold (p<0.0001) (Figure 5D) and developed dysmorphic cristae during treatment (Figure 5E). In parallel, tenofovir also caused statistical-

ly significant inhibition of PNTP1 and ATP6 mRNA expression in vaginal epithelial cells (Figure 5F).

Proteomics of rectal secretions corroborates enhancing effect of tenofovir on cell survival

Extensive protein studies were not an intended part of MTN-007 and samples were not preserved optimally for this purpose. However, 483 proteins were detected consistently at baseline and time point VII by mass spectrometry. 382 proteins increased in the tenofovir arm versus 112 in the no treatment arm (5 participants/arm). Among these, significant increases in individual protein expression were only seen in the tenofovir arm (Figure S7A). The top 100 proteins exhibited an average fold increase of 3.8 (median 3.2, range 1.6-128.7) in the tenofovir arm, listed by p value in Figure S7B. Enrichment analysis primarily indicated enhancement of cell survival and induction of leukocyte migration by tenofovir (Figure S7C), which is consistent with our other findings.

Discussion

Our findings indicate that reduced glycerin rectal tenofovir 1% gel affects expression of a different and much broader range of genes than N-9 2% gel, potentially impairing mucosal immune homeostasis, mitochondrial function, and regulation of epithelial cell differentiation and survival. These results make bio-

Figure 5. Quantification of mitochondria-associated parameters

A PNPT1 mRNA copy numbers measured in 9 and 15 cm biopsies at baseline (0), after a single tenofovir gel application (I) and after seven consecutive once-daily applications (VII) by RT-ddPCR assay.

B Mitochondrial ATP6 mRNA copy numbers measured in 9 cm biopsies after tenofovir or N-9 treatment. Line colors in (a) and (b) signify the 15 participants in the tenofovir arm. Black lines signify the 15 participants in the N-9 arm. Baseline values were compared between 9 and 15 cm biopsies by paired t-test and between tenofovir and N-9 by unpaired t-test. Expression changes over time were tested for statistical significance by ANOVA with Bonferroni adjusted post-tests.

C Assessment of mitochondrial density by electron microscopy of 9 cm biopsies in two study participants. Each dot indicates the mean number of mitochondria per μm^2 in a separate 2,000× image.

D Assessment of mitochondrial sizes by electron microscopy in the same biopsies. Each dot depicts the size in μm^2 of an individual mitochondrion measured at 5,000×. Dot colors in (C) and (D) correspond to the line colors of the same two study participants in (A) and (B). Density and size changes were tested for statistical significance by unpaired t-tests. Horizontal lines and error bars depict means and standard deviations.

E Representative electron microscopy images of normal mitochondria at baseline, and of enlarged and dysmorphic mitochondria at time point VII, in 9 cm biopsies of Subject Y. Fine structural detail is limited due to formalin fixation of biopsies.

F PNPT1 and ATP6 gene expression in vaginal epithelial cell cultures in response to 1 and 7 days of 50 μM (blue boxes) or 500 μM (green boxes) tenofovir exposure *in vitro*. Boxes and error bars signify means and standard
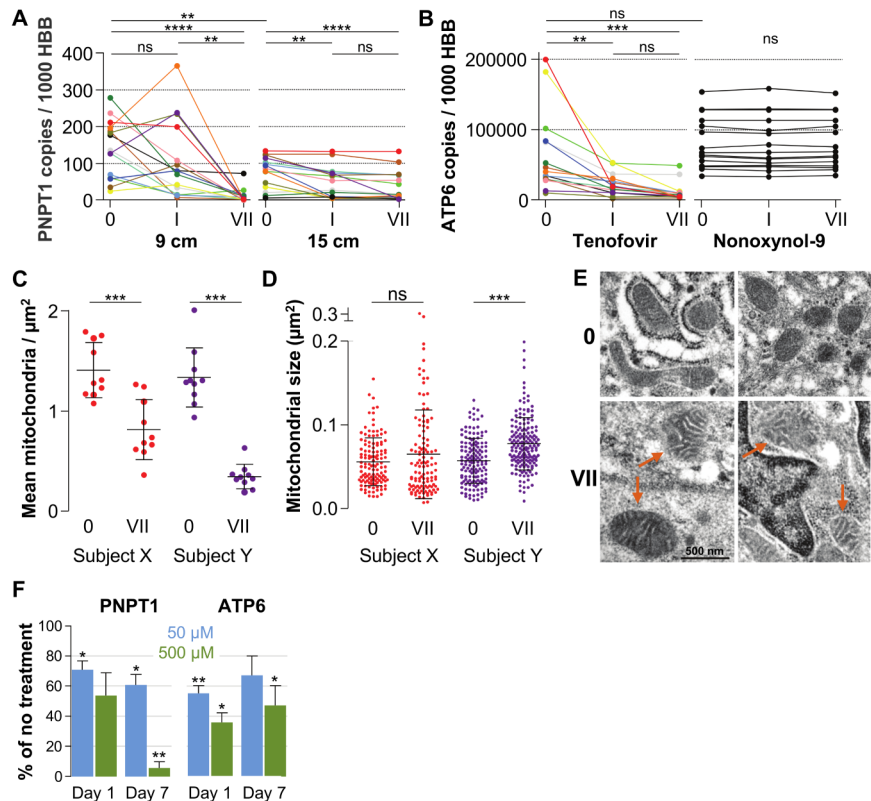
deviations across four independent experiments with epithelial cell cultures derived from the vaginal mucosa of four healthy women. Statistical significance levels in all figure panels are indicated by asterisks (*, p<0.05; **, p<0.01; ***, p<0.001; ****, p<0.0001; "ns", not significant).

logical sense given that tenofovir is a DNA chain terminator, with possible off-target effects in human cells[35], and that topical application achieves at least one hundred-fold higher active drug concentrations in the mucosa than oral administration of 300 mg tenofovir disoproxil fumarate[7,36]. Moreover, tenofovir caused similar changes in primary vaginal epithelial cells cultured from several healthy women.

We did not find evidence that tenofovir directly causes inflammation. Rather, tenofovir dampened anti-inflammatory factors. Most prominently, it strongly inhibited IL-10 gene and protein expression, likely via blocking of CREB1 and its coactivator CREBBP[26,27,37,38]. In addition, it compromised signaling pathways downstream of TGF-β, a central anti-inflammatory mediator in the gut[39,40]. Consequently, a number of chemokines were induced, such as the B lymphocyte chemo-attractant CXCL13[41], and CCL19 and CCL21, both ligands of CCR7 on T lymphocytes and dendritic cells[42]. Correspondingly, CCR7, the B cell marker CD19, and the T cell markers CD2, CD3D and CD7 increased. In keeping with this, we observed higher densities of CD3+ and CD7+ T lymphocytes in the rectal mucosa following seven days of tenofovir 1% gel use. In concert, these changes suggest that tenofovir creates a state of potential hyper-responsiveness to external inflammatory stimuli but does not itself cause inflammation. In populations with a high incidence of mucosal infections and associated immune activation, this could potentially negate the antiviral protective effect of topical tenofovir prophylaxis[43]. Intriguingly, recent findings in CAPRISA 004 participants support this notion: while pericoital vaginal tenofovir was overall protective[1], inflammation increased the risk of HIV infection much more in the tenofovir arm than in the placebo arm (Passmore JA et al.; submitted).

Mitochondrial toxicity of nucleotide/nucleoside reverse transcriptase inhibitors such as tenofovir is well described but the mechanism remains unclear[35]. We found that tenofovir strongly and consistently inhibited expression of PNPT1, which encodes polynucleotide phosphorylase (PNPASE). PNPASE regulates nucleus-encoded RNA import into mitochondria[29]. In PNPT1 knock-out mice, mitochondrial morphology and respiratory capacity is disrupted in a manner quite similar to the disruption in renal proximal tubular cells in patients with tenofovir-induced nephrotoxicity[29,44]. Strikingly, in our study, just one week of daily tenofovir 1% gel application greatly lowered transcription of mitochondrial ATP6 and caused visible ultrastructural mitochondrial changes. These findings suggest that tenofovir's suppression of PNPT1 expression may underlie its reported, but heretofore unexplained, mitochondrial toxicity.

A number of changes in rectal biopsies and primary vaginal epithelial cells also suggested that tenofovir can cause epithelial hyper-proliferation. Furthermore, tenofovir's negative effect on mitochondrial function could lead to impairment of tumor progenitor cell apoptosis[45,46], as has been specifically reported for loss-of-function mutations of mtATP6, a mitochondrial gene strongly suppressed by tenofovir in our study[47]. Neoplastic pressure could also arise from the strong induction of KIAA0101 and UBD (ubiquitin D). KIAA0101 is important for regulation of DNA repair[48], is increased in tumor tissues[31], and enhances cancer cell growth[32,49]. UBD appears to increase mitotic non-disjunction and chromosome instability[50,51], and is highly up-regulated in gastrointestinal cancers[33,50,51]. Notably, though, these findings remain circumstantial, as there is no actual clinical evidence for carcinogenicity. Nevertheless, they raise the question of whether the relatively high concentrations of tenofovir achieved in the mucosa during topical use could potentially lead to neoplastic lesions with continuous and long-term use. According to Viread's Product Monograph, gastrointestinal tumorigenicity has been observed in mice after high oral dosing of tenofovir disoproxil fumarate. Vaginal tumorigenicity has been documented for azido-thymidine, an NRTI and DNA chain terminator like tenofovir, which induced vaginal hyperplasia and carcinomas when delivered to mice intravaginally as a 2% solution (~25% carcinoma rate)[52].

This is the first time that a systems biology approach has been applied to a clinical trial of mucosal pre-exposure prophylaxis and our study shows the value of using these technologies for comprehensive mucosal safety assessment. Our findings raise concerns regarding the safety of topical tenofovir 1% gel in the rectum. Tenofovir's effects on vaginal epithelial cells suggest similar activities in the vagina, which we will verify in MTN-014, an upcoming phase I clinical trial comparing vaginal and rectal tenofovir 1% gel in a cross-over format. Further studies are required to gauge whether tenofovir, which has become a valuable cornerstone drug in treating HIV infection, can also be safely and effectively used as a vaginal or rectal microbicide.

Methods

Design of the Clinical Study

MTN-007 (ClinicalTrials.gov registration NCT01232803) was a phase 1, double blind, placebo-controlled trial in which participants were randomized to receive rectal reduced glycerin tenofovir 1%, nonoxynol-9 (N-9) 2% or hydroxyethylcellulose (HEC) gels, or no-treatment (1:1:1:1), at three clinical research sites (Pittsburgh, PA; Birmingham, AL; and Boston, MA). The study protocol was approved by IRBs at all three sites. All participants gave written informed consent. The study details, and general safety and acceptability data, have been published elsewhere and showed that rectal tenofovir 1% gel was well tolerated and appeared safe by established safety parameters[3]. Each gel was administered as a single dose and then, after at least a one-week recovery period, once daily for seven consecutive days. The first dose of study product was self-administered under supervision by the clinic staff at the Treatment 1 Visit. Subsequent administrations occurred at home, and study participants were instructed to insert one dose of gel into the rectum once daily throughout the 7-day period in the evening or before the longest period of rest.

Study Participants and Products

A total of 65 study participants were enrolled and randomized in the study, 62 of whom completed it (tenofovir, n = 15; N-9, n = 16; HEC, n = 15; and no treatment, n = 16). Forty-three (69%) were male. Microarray studies were performed on eight randomly selected male participants in each group, and confirmatory gene expression studies were done on the remaining participants.

The study population consisted of healthy, HIV-uninfected adults aged 18 or older who were required to abstain from receptive anal intercourse during the course of the clinical trial. Female participants were required to use effective contraception. Individuals with abnormalities of the colorectal mucosa, significant gastrointestinal symptoms (such as a history of rectal bleeding or inflammatory bowel disease), evidence of anorectal Chlamydia trachomatis or Neisseria gonorrhea infection, hepatitis B infection, or who used anticoagulants were excluded from the study. Reduced glycerin tenofovir 1% gel and HEC gel, known as the "Universal Placebo Gel"[4], were supplied by CONRAD (Arlington, VA, USA). 2% N-9 gel was provided as Gynol II® (Johnson & Johnson). All study products were provided in identical opaque HTI polypropylene pre-filled applicators (HTI Plastics) containing 4 mL of study product.

Mucosal Biopsy Procedures

Rectal biopsies for the microarray studies were obtained before treatment at enrollment (time point "0"), 30-60 minutes following application of the single gel dose (time point "I"), and again on the day following the last dose of the seven once-daily gel applications (time point "VII"). Following an enema with Normosol-R pH 7.4, a flexible sigmoidoscope was inserted into the rectum and biopsies were collected at 15 cm from the anal margin. Following the sigmoidoscopy, a disposable anoscope was inserted into the anal canal for collection of rectal biopsies at 9 cm from the anal margin. Immediately after harvest, biopsies were immersed in RNAlater (Qiagen), stored at 4°C overnight and transferred to a -80°C freezer for long-term storage until shipping to Seattle and processing.

Primary Vaginal Keratinocyte Cultures

Tissues routinely discarded from vaginal repair surgeries were harvested from four otherwise healthy adult women, placed in ice-cooled calcium- and magnesium-free phosphate-buffered saline containing 100 U/ml penicillin, 100 µg/ml streptomycin and 2.5 µg/ml Fungizone (Life Technologies), and transported to the laboratory within 1 hr of removal from the donor. Tissue harvesting and experimental procedures were approved by the Institutional Review Boards of the University of Washington and the Fred Hutchinson Cancer Research Center. The deep submucosa was removed with surgical scissors and the remaining vaginal mucosa was cut into 5 x 5 mm pieces, which were incubated at 4°C for 18 hr in 5 ml of a 25 U/ml dispase solution (354235; BD Biosciences). The epithelial sheets were dissected off under a stereoscope and incubated for 10-12 min at 37°C in 2 ml 0.05% trypsin while gently shaking. The dispersed cells were poured through a 100 µm cell strainer into a 50 ml tube, pelleted by centrifugation, and resuspended in F medium (3:1 [v/v] F12 [Ham]-DMEM [Life Technologies], 5% fetal calf serum [Gemini Bio-Products], 0.4 µg/ml hydrocortisone [H-4001; Sigma], 5 µg/ml insulin [700-112P; Gemini Bio-Products], 8.4 ng/ml cholera toxin [227036; EMD Millipore], 10 ng/ml epidermal growth factor [PHG0311; Life Technologies], 24 µg/ml adenine [A-2786; Sigma], 100 U/ml penicillin, and 100 µg/ml streptomycin [Life Technologies]). The keratinocytes were plated into culture flasks in the presence of ~12,500/cm^2 irradiated (6000 Rad) 3T3-J2 feeder fibroblasts (a kind gift by Cary A. Moody) and 10 µM of Rho kinase inhibitor Y27632 (1254; Enzo Life Sciences) was added[5,6]. Keratinocytes were fed every 2-3 days and passaged when around 80% confluent by 1 min treatment with 10 ml versene (Life Technologies) to remove the feeder cells, followed by 5 min treatment with trypsin/EDTA (Life Technologies). Dislodged keratinocytes were washed and re-plated at ~2,500 keratinocytes/cm^2 with irradiated 3T3-J2 feeder fibroblasts.

Tenofovir Treatment of Primary Vaginal Keratinocytes

Tenofovir (CAS 147127-20-6; T018500, Toronto Research Chemicals) was dissolved in phosphate-buffered saline, 7% dimethyl sulfoxide and 5% 5N sodium hydroxide to result in a 767 mM stock solution, and further diluted in culture media for addition to keratinocyte cultures in concentrations ranging from 0.05 to 32 mM. Based on initial titration experiments in which we measured the intracellular concentration of tenofovir diphosphate, the active cellular metabolite of tenofovir, by liquid chromatography-tandem mass spectrometry (performed in the laboratory of Dr. Craig Hendrix, Johns Hopkins University), concentrations in the culture media at the lower end (0.05 to 0.5 mM range) were estimated to be equivalent to the active concentrations likely achieved by topical tenofovir 1% gel (35 mM) in mucosal epithelial cells in

vivo[7,8]. In all experiments, control keratinocytes were cultured in parallel without tenofovir. Keratinocytes were harvested at pre-determined time points, split into several aliquots, and pelleted. Pellets were frozen and stored at -80°C either as dry pellets for protein assays or after suspension in RNAprotect Cell Reagent (Qiagen) for RNA assays.

AlamarBlue Cell Proliferation and Cell Viability Assay

Primary vaginal keratinocytes were cultured in 6-well plates (Corning) with or without various concentrations of tenofovir for up to 14 days. At day 1, day 4, day 7 or day 14 the alamarBlue reagent (BUF012A; AbD Serotec) was added. After 5 hours, absorbance was measured at 570 and 600 nm on a Varioskan Flash Multimode reader (Thermo Scientific). Percentage reduction of alamarBlue, corresponding to the level of cell proliferation, was calculated as specified in the manufacturer's technical datasheet. This was converted to percentage of maximal alamarBlue reduction by dividing each well by the well with the highest amount of alamarBlue reduction.

Interleukin-10 ELISA Assay

The IL-10 concentration in primary vaginal keratinocytes was measured after lysis of frozen cell pellets in Cell Lysis buffer (R&D Systems) using a commercial human IL-10 immunoassay (Quantikine HS, HS100C; R&D Systems) according to the manufacturer's specifications.

RNA isolation, cRNA Preparation and Whole Genome BeadArray Hybridization

RNA was isolated from the biopsies using the RNeasy Fibrous Tissue Mini Kit (Qiagen), and from the vaginal keratinocytes using the Direct-zol RNA MiniPrep kit (Zymo Research), according to the manufacturer's instructions, treated with 27 Kunitz units of DNAse (Qiagen) to remove genomic DNA contamination, and evaluated for integrity using the Agilent RNA 6000 Nano Kit (Agilent, Palo Alto, CA) on an Agilent 2100 Bioanalyzer. All samples had an RNA Integrity Number of 7 or greater. 500 ng of total RNA was amplified and labeled using the Illumina TotalPrep RNA Amplification kit (Ambion). cRNA from a total of 192 rectal biopsy samples (8 men per study arm, 4 study arms, 3 time points and 2 biopsy sites [9 cm and 15 cm]), and from a total of 36 primary vaginal keratinocyte cultures (3 tissue donors, 3 arms and 4 time points), was hybridized to HumanHT12 v4 Expression BeadChips (Illumina) according to the manufacturer's protocols. Each chip contains 47,323 probes, corresponding to 30,557 genes.

Unbiased Mass Spectrometry of Rectal Sponge Eluates

Protein concentration of rectal eluates was determined by BCA assay (Novagen). Equal amounts of total protein from each sample (100 µg) were then denatured in pH 8.0 urea exchange buffer (8 M Urea [GE HealthCare], 50 mM HEPES [Sigma]) for 20 minutes at room temperature, and then placed into 10 kDa Nanosep filter cartridges. After centrifugation, samples were treated with 25mM dithiothreitol (Sigma) for 20 minutes, then 50mM iodoacetamide (Sigma) for 20 minutes, followed by a wash with 50mM HEPES buffer. Trypsin (Promega) was added (2 µg/100 µg protein) and samples were incubated at 37°C overnight in the cartridge. Peptides were eluted off the filter with 50 mM HEPES, and the digestion was stopped with 1% formic acid. Peptides were dried via vacuum centrifugation and cleaned of salts and detergents by reversed-phase liquid chromatography (high pH RP, Agilent 1200 series micro-flow pump, Water XBridge column) using a step-function gradient. The fractions were then dried via vacuum centrifugation. Equal amounts of peptides were re-suspended in 2% acetonitrile (Fisher Scientific), 0.1% formic acid (EMD Canada) and injected into a nano-flow LC system (Easy nLC, ThermoFisher) connected in-line to a LTQ Orbitrap Velos mass spectrometer (Thermo Fisher). Mass spectrometry instrument settings were the same as described previously[9].

Quality Control and Processing of Microarray and Mass Spectrometry Data

Microarray Data

All chips used in the analysis passed standard quality control metrics assessed by GenomeStudio (Illumina) as well as visual inspection for anomalies and artifacts. GenomeStudio calculates a detection p value for each probe, which represents the confidence that a given transcript is expressed above back-

ground defined by negative control probes. Further processing and statistical analysis of data was done using the R/Bioconductor software suite[10]. Data were pre-processed by robust spline normalization and variance stabilizing transformation using the Bioconductor lumi package[11,12]. The pre-processed data were filtered to include only probes with detection threshold p values of < 0.05 in 100% of biopsies in at least one of the four study arms, or in 100% of vaginal epithelial cell cultures, and to remove probes that had a low standard deviation (≤ 0.5) across all arrays, using the Bioconductor genefilter package[13]. Finally, probes without an Entrez ID were removed, leaving 1,928 probes in the rectal biopsies, and 6,699 probes in the vaginal epithelial cell cultures, for further statistical analysis.

Mass Spectrometry Data

All spectra were processed using Mascot Distiller v2.3.2 (Matrix Science), against the UniProtKB/SwissProt (2012-05) Human (v3.87) database using the decoy database option (2% false discovery rate), along with the following parameters: carbamidomethylation (cysteine residues) (K and N-terminus) as fixed modifications, oxidations (methionine residues) as a variable modification, fragment ion mass tolerance of 0.5 Da, parent ion tolerance of 10 ppm, and trypsin enzyme with up to 1 missed cleavage. Mascot search results were imported into Scaffold (v4.21) (Proteome Software) and filtered using 80% confidence for peptides, 99% confidence for proteins, and at least 2 peptides per protein. Label-free protein expression levels based on MS peak intensities were calculated using Progenesis LC-MS software (v4.0 Nonlinear Dynamics). Feature detection, normalization and quantification were all performed using default settings in the software. Retention time alignment was performed using automatic settings and manually reviewed for accuracy on each sample. Only charge states between 2+ and 10+ were included. Protein abundances were further normalized by total ion current.

Statistical Analysis of Microarray and Mass Spectrometry Data

Microarray Data

A Bayesian statistical framework, Cyber-T[14,15], was run from the CyberT/hdarray library in R to test for the effect of tenofovir treatment on gene expression. The effect of tenofovir 1% gel on the rectal mucosa in vivo was tested in paired comparisons between time point I or VII and time point 0. Each study arm was considered separately. The effect of tenofovir on vaginal epithelial cell cultures in vitro was tested in paired comparisons between treated and untreated cultures. Each tenofovir dosage (50 and 500 μM) and time point (1, 4, 7 and 14 days) was considered separately. The Benjamini & Hochberg method for estimating false discovery rates (FDR) was used to control for multiple comparisons[16]. Criteria for significance and relevance were an estimated FDR ≤ 0.05 and a $\log_2$ fold expression change of ≥ 0.5 (induction) or ≤ -0.5 (suppression), respectively. For confirmation and to control for the potential time effect in this longitudinal study, the normalized but unfiltered data (all 47,323 probes) were also analyzed for significant treatment effects using a double subtraction strategy, where the paired differences between time point 0 and time points I or VII within each treatment arm were first calculated for each probe and study participant. In a second step, the mean paired differences for each probe within each of the three treatment arms were compared to mean paired differences for each probe within the no-treatment arm. Analysis for significance was performed via a linear fit model using the limma package[17], with the same significance criteria used for Cyber-T. The resulting gene lists greatly overlapped with the Cyber-T results. For simplicity, the numbers of induced and suppressed genes reported in Results are based on the Cyber-T analysis. Heat maps of differentially regulated genes were generated using MeV 4.8 within the TM4 Microarray Software Suite[18], and hierarchically clustered according to selected gene ontologies found in the databases DAVID 6.7[19] and InnateDB[20]. All microarray data were deposited into the GEO database (accession numbers GSE57025 and GSE57026).

Mass Spectrometry Data

Protein intensity values were log transformed to mean expression values across all samples. To evaluate time-induced effects in the tenofovir gel arm, paired protein abundance values in each subject were normalized to time point 0 from time point VI. Statistical analysis for differences between the two time points was done by paired t tests.

Pathway and Network Analysis of Microarray and Mass Spectrometry Data

Microarray Data

Entrez ID designations, assigned to the array probes by Illumina, were uploaded to the Innate DB database and a Gene Ontology (GO) over-representation analysis was performed for gene groups signifying a particular molecular function or biological process, or occurring in specific cellular compartments[20]. The following strategy was used to determine which gene groups were enriched in the data set: separately for suppressed and induced genes, ratios of the number of genes in a particular GO group to the total number of genes detected in our data set were compared to the ratios in the same GO group reported for the complete human genome using Fisher's exact test. Ingenuity Pathways Analysis (IPA) (Ingenuity Systems) was used to visualize direct and indirect relationships between individual gene products and map their cellular localizations.

Mass Spectrometry Data

Proteomic data were uploaded into the IPA software package (Ingenuity Systems). Associations between protein groups in the dataset and canonical pathways were measured similarly to the over-representation analysis described for the microarray data above. IPA software was also used to compare protein expression patterns against the IPA biological function database. IPA software calculates a Benjamini & Hochberg-adjusted p-value for the association of protein abundance changes with each biological function, and a weighted z-score, which estimates whether the protein abundance changes found associated with a specific biological function are likely to enhance (positive z values) or inhibit (negative z values) the function.

Quantitative Confirmation of Microarray Results by RT-ddPCR

A two-step reverse transcription (RT) droplet digital PCR (ddPCR) was used to confirm microarray transcriptome data for selected genes of interest[21,22]. In a ddPCR assay, each sample is partitioned into ~20,000 droplets representing as many individual PCR reactions. The number of target DNA copies present per sample can be quantified based on Poisson distribution statistics, because each individual droplet is categorized as positive or negative for a given gene. For rectal biopsies, cDNA was generated using the High Capacity cDNA Reverse Transcription Kit (Life Technologies) and the ddPCR was carried out using the 2X ddPCR Supermix for Probes (BioRad). For epithelial cell lines, these steps were combined using the 2X One-Step RT-ddPCR Kit for Probes (BioRad). ddPCR was performed on the QX100 droplet digital PCR system (BioRad). Reactions were set up with 20X 6-carboxyfluorescein (FAM)-labeled target gene-specific qPCR assay (Integrated DNA Technologies or Life Technologies) and 20X VIC-labeled housekeeping hemoglobin B (HBB) gene-specific Taqman gene expression assay (Life Technologies). Each assembled ddPCR reaction mixture was loaded in duplicate into the sample wells of an eight-channel disposable droplet generator cartridge (BioRad) and droplet generation oil (BioRad) was added. After droplet generation, the samples were amplified to the endpoint in 96-well PCR plates on a conventional thermal cycler using the following conditions: denaturation/enzyme activation for 10 min at 95°C, 40 cycles of 30 sec denaturation at 94°C and 60 sec annealing/amplification at 60°C, followed by a final 10 min incubation step at 98°C. After PCR, the droplets were read on the QX100 Droplet Reader (BioRad). Analysis of the ddPCR data was performed with QuantaSoft analysis software version 1.3.1.0 (BioRad).

Immunohistochemistry of Formalin-Fixed Rectal Biopsies

Four-micron sections were cut on a Leica RM2255 Automated Rotary Microtome (Leica), mounted on positively charged EP-3000 slides (Creative Waste Solutions), dried for 1 hr at 60°C, and stored until staining at 4°C. Slides were deparaffinized in xylene and rehydrated in graded dilutions of ethanol in water. Antigen retrieval was performed by heating the slides in Trilogy™ Pretreatment Solution (Cell Marque) for 20 min at boiling temperature in a conventional steamer (Black&Decker). Slides were then cooled for 20 min, rinsed three times in Tris-buffered 0.15 M NaCl solution containing 0.05% Tween 20 (Wash Buffer; Dako), and stained at room temperature in an automated slide-processing system (Dako Autostainer Plus). Endogenous peroxide activity was blocked using 3% H2O2 for 8 min, followed by 10 min in Serum-Free Protein Block (Dako). The slides were then stained for one hour with the

primary antibodies. Staining was performed with the following primary antibodies: anti-CD3 (RM9107S, rabbit clone SP7; Lab Vision Corporation), anti-ubiquitin D (NBP2-13498, rabbit polyclonal anti-FAT10 antibody; Novus Biologicals), anti-CD7 (M7255, mouse clone CBC.37; Dako), and anti-interleukin-10 (sc-8438, mouse clone E-10; Santa Cruz Biotechnology). Negative control primary immunoglobulins were either whole rabbit IgG (011-000-003; Jackson ImmunoResearch Laboratories) or mouse IgG (I-2000; Vector Laboratories).

For CD3 staining, the slides were incubated with anti-CD3 for 60 min at a dilution of 1:25, washed in Wash Buffer, incubated for 30 min with sheep-anti-rabbit Dylight 649 (611-643-122; Rockland Immunochemicals), washed, and incubated for 30 min with donkey-anti-sheep Dylight 649 (613-743-168; Rockland). Sections were counter-stained for 20 min with the nucleic acid-binding dye Sytox Orange (S11368; Life Technologies) at a dilution of 1:20,000, and coverslipped in ProLong Gold antifade reagent (P36930; Life Technologies). For ubiquitin D (UBD), CD7 and interleukin-10 (IL-10) staining, the slides were incubated with 0.8 µg/ml (UBD and CD7) or 4 µg/ml (IL-10) of the primary antibody for 60 min. After washing, the anti-UBD stained slides were incubated for 30 min with Leica Power Vision HRP rabbit specific polymer (PV6119; Leica Biosystems); and the anti-CD7 and anti-IL-10 stained slides were incubated for 30 min with Leica Power Vision HRP mouse specific polymer (PV6114; Leica Biosystems). After washing, staining was visualized with 3,3'-diaminobenzidine (Liquid DAB+ Substrate Chromogen System; Dako) for 7 minutes, and the sections were counter-stained for 2 min with hematoxylin (Biocare). Controls for all antibodies were run with identical procedures but replacing the primary antibodies with either rabbit IgG or mouse IgG, as appropriate, at calculated matching concentrations.

Acquisition and Analysis of Stained Tissue Sections

Sequences of slightly overlapping 20X (for CD3, UBD or CD7) or 40X (for IL-10) images covering each stained tissue section in its entirety were acquired on a bright-field Aperio Scanscope AT (for UBD, CD7 and IL-10) or a fluorescent Aperio Scanscope FL (for CD3) (Aperio ePathology Solutions, Leica Biosystems). Overlapping images were stitched together using the Aperio Image Analysis Suite, and the entire tissue sections on each slide were analyzed using Definiens Tissue Studio (Definiens AG). Individual cells were identified based on the nuclear counter-stain. For CD3 and CD7, all positive cells were automatically counted and reported as number of positive cells per mm^2 of tissue section. For IL-10 and UBD, tight regions were manually drawn around all areas of the tissue sections containing columnar epithelial cells. For IL-10, all positive columnar epithelial cells were automatically counted and reported as number of positive cells per mm^2. For UBD, which stained all epithelial cells, the mean staining intensity (MSI) of each columnar epithelial cell was measured in arbitrary units and overall UBD staining intensity for each section was reported as the average MSI of all epithelial cells.

Electron Microscopy

Formalin-fixed paraffin-embedded rectal biopsies were de-paraffinized and fixed overnight in half-strength Karnovsky's fixative. Staining, embedding, cutting and viewing on a JEOL 1400 SX transmission electron microscope were performed as previously described[23,24]. Twenty images per sample were acquired at 5,000X magnification. Using ImageJ[25], the 2-dimensional sizes in $µm^2$ of all individual mitochondria with a circularity index of ≥ 0.9 were calculated (for standardization purposes, only mitochondria cut near perfectly along their minor axis were evaluated). Ten images per sample were also acquired at 2,000X magnification, always including the epithelial cell brush border. Using ImageJ, a grid of 1.32 $µm^2$ squares of defined size was overlaid onto each image. All mitochondria in the images were counted, except those in the first row of squares falling on the brush border and in squares along the image rims which only partially covered tissue), and the mean numbers of mitochondria per $µm^2$ were calculated for each of the acquired 2,000X images (range of counted squares per image: 23 to 50). Mitochondrial sizes and mean numbers per $µm^2$ were compared between time point 0 and time point VII using unpaired two-sided t tests.

General Statistics

All p values reported were adjusted for multiple testing as appropriate, except for the exploratory protein mass spectrometry data. Correlations of $\log_2$ fold gene expression changes between 9 cm and 15 cm biopsies in Figure 1C and Figure S1 were tested by Spearman's rank correlation coefficient. Gene and protein expression changes over baseline were compared between study arms by two-tailed Mann-Whitney test (Figure S2 and S7). The combined expression data from the microarray and RT-ddPCR tests shown in Figure 2C were compared separately for log-fold induction or suppression over baseline using a one-tailed Wilcoxon signed-rank test with Bonferroni adjustment. Immuno-histology measurements in Figure 2D were compared between baseline and after seven days of treatment by two-tailed paired t tests. Due to high skewness of the $CD7^+$, $CD3^+$ and $IL-10^+$ cell counts, these were tested after $\log_{10}$ transformation. Ratios of induced to suppressed genes in Figure 3A were tested for a difference between cellular compartments using Chi-square statistics. DSP, IL-10, KIAA0101, PNPT1 and ATP6 copy numbers or protein concentrations in Figure 4B, 4C, 5A, 5B and 5G were tested for significant change across three time points by repeated measures ANOVA, and exact Bonferroni-adjusted post-tests were run for comparisons between two time points. Due to high skewness of the KIAA0101 copy numbers, these were tested after $\log_{10}$ transformation. The effect of increasing tenofovir concentrations on the proliferation of primary vaginal epithelial cells in Figure 4D was assessed for significance by a linear model accounting for days and donors. Copy numbers between 9 cm and 15 cm biopsies in Figure 5A were compared by two-tailed paired t test. Copy numbers between baseline tenofovir and N-9 in Figure 5B were compared by a two-tailed unpaired t test. Mitochondria counts and sizes in Fig. 5D and D were compared between baseline and Day VII by two-tailed unpaired t tests. Microarray chip probe expression values were tested for correlation between the three primary vaginal cell cultures by computing pairwise Pearson correlation coefficients (Table S1). Statistics packages used were Prism 6 (Graphpad Software) and Bioconductor/Lumi in R.

Acknowledgements

Author Contributions

FH, LB, JD, MJM and IM designed the microarray study. FH and LB developed microarray technologies. LB carried out microarray and RT-ddPCR experiments. AB and TBB carried out the protein mass spectrometry experiments. LV, JS, LB and FH carried out the electron microscopy experiments. LB and LV established the primary epithelial cell cultures. CH, RDC, and KHM recruited study participants and acquired participant data. FH, LB, JD, SF, RG and MJC analyzed the gene expression data. CH, PA, SJ, RDC and KHM provided operational support for the clinical study. JP advised on all aspects of the study. DRF provided the study drug. IM designed the clinical trial. FH is the principal author of this manuscript, and LB, SH, MJM and IM contributed to writing the manuscript.

Funding

1 Abdool Karim Q, Abdool Karim SS, Frohlich JA, Grobler AC, Baxter C, et al. (2010) Effectiveness and safety of tenofovir gel, an antiretroviral microbicide, for the prevention of HIV infection in women. Science 329: 1168-1174.

2 Marrazzo J, Ramjee G, Nair G, Palanee T, Mkhize B, et al. (2013) Pre-exposure prophylaxis for HIV in women: daily oral tenofovir, oral tenofovir/emtricitabine, or vaginal tenofovir gel in the VOICE study (MTN 003). 20th Conference on Retroviruses and Opportunistic Infections. Atlanta. pp. 26LB.

3 McGowan I, Hoesley C, Cranston RD, Andrew P, Janocko L, et al. (2013) A phase 1 randomized, double blind, placebo controlled rectal safety and acceptability study of tenofovir 1% gel (MTN-007). PLoS ONE 8: e60147.

4 Tien D, Schnaare RL, Kang F, Cohl G, McCormick TJ, et al. (2005) In vitro and in vivo characterization of a potential universal placebo designed for use in vaginal microbicide clinical trials. AIDS Res Hum Retroviruses 21: 845-853.

5 Chapman S, Liu X, Meyers C, Schlegel R, McBride AA (2010) Human keratinocytes are efficiently immortalized by a Rho kinase inhibitor. J Clin Invest 120: 2619-2626.

6 Liu X, Ory V, Chapman S, Yuan H, Albanese C, et al. (2012) ROCK inhibitor and feeder cells induce the conditional reprogramming of epithelial cells. Am J Pathol 180: 599-607.

7 Hendrix CW, Chen BA, Guddera V, Hoesley C, Justman J, et al. (2013) MTN-001: randomized pharmacokinetic cross-over study comparing tenofovir vaginal gel and oral tablets in vaginal tissue and other compartments. PLoS ONE 8: e55013.

8 Louissaint NA, Cao YJ, Skipper PL, Liberman RG, Tannenbaum SR, et al. (2013) Single Dose Pharmacokinetics of Oral Tenofovir in Plasma, Peripheral Blood Mononuclear Cells, Colonic and Vaginal Tissue. AIDS Res Hum Retroviruses.

9 Burgener A, Tjernlund A, Kaldensjo T, Abou M, McCorrister S, et al. (2013) A systems biology examination of the human female genital tract shows compartmentalization of immune factor expression. J Virol 87: 5141-5150.

10 Gentleman RC, Carey VJ, Bates DM, Bolstad B, Dettling M, et al. (2004) Bioconductor: open software development for computational biology and bioinformatics. Genome Biol 5: R80.

11 Du P, Kibbe WA, Lin SM (2008) lumi: a pipeline for processing Illumina microarray. Bioinformatics 24: 1547-1548.

12 Lin SM, Du P, Huber W, Kibbe WA (2008) Model-based variance-stabilizing transformation for Illumina microarray data. Nucleic Acids Res 36: e11.

13 Bourgon R, Gentleman R, Huber W (2010) Independent filtering increases detection power for high-throughput experiments. Proc Natl Acad Sci U S A 107: 9546-9551.

14 Baldi P, Long AD (2001) A Bayesian framework for the analysis of microarray expression data: regularized t -test and statistical inferences of gene changes. Bioinformatics 17: 509-519.**15** Long AD, Mangalam HJ, Chan BY, Tolleri L, Hatfield GW, et al. (2001) Improved statistical inference from DNA microarray data using analysis of variance and a Bayesian statistical framework. Analysis of global gene expression in Escherichia coli K12. J Biol Chem 276: 19937-19944.

16 Benjamin Y, Hochberg Y (1995) Controlling the false discovery rate: A practical and powerful approach to multiple testing. Journal of the Royal Statistical Society, Series B (Methodological) 57: 289-300.

17 Smyth GK (2005) Limma: linear models for microarray data. In: Gentleman R, Carey V, Dudoit S, Irizarry R, Huber W, editors. Bioinformatics and Computational Biology Solutions using R and Bioconductor. New York: Springer. pp. 397-420.

18 Saeed AI, Bhagabati NK, Braisted JC, Liang W, Sharov V, et al. (2006) TM4 microarray software suite. Methods Enzymol 411: 134-193.

19 Huang da W, Sherman BT, Lempicki RA (2009) Systematic and integrative analysis of large gene lists using DAVID bioinformatics resources. Nat Protoc 4: 44-57.

20 Lynn DJ, Winsor GL, Chan C, Richard N, Laird MR, et al. (2008) InnateDB: facilitating systems-level analyses of the mammalian innate immune response. Mol Syst Biol 4: 218.

21 Hindson BJ, Ness KD, Masquelier DA, Belgrader P, Heredia NJ, et al. (2011) High-throughput droplet digital PCR system for absolute quantitation of DNA copy number. Anal Chem 83: 8604-8610.

22 Pinheiro LB, Coleman VA, Hindson CM, Herrmann J, Hindson BJ, et al. (2012) Evaluation of a droplet digital polymerase chain reaction format for DNA copy number quantification. Anal Chem 84: 1003-1011.

23 Hladik F, Sakchalathorn P, Ballweber L, Lentz G, Fialkow M, et al. (2007) Initial events in establishing vaginal entry and infection by human immunodeficiency virus type-1. Immunity 26: 257-270.

24 Hladik F, Lentz G, Akridge RE, Peterson G, Kelley H, et al. (1999) Dendritic cell-T-cell interactions support coreceptor-independent human immunodeficiency virus type 1 transmission in the human genital tract. J Virol 73: 5833-5842.

25 Collins TJ (2007) ImageJ for microscopy. Biotechniques 43: 25-30.

26 Alvarez Y, Municio C, Alonso S, Sanchez Crespo M, Fernandez N (2009) The induction of IL-10 by zymosan in dendritic cells depends on CREB activation by the coactivators CREB-binding protein and TORC2 and autocrine PGE2. J Immunol 183: 1471-1479.

27 Woodgett JR, Ohashi PS (2005) GSK3: an in-Toll-erant protein kinase? Nat Immunol 6: 751-752.

28 Neuhofer W (2011) Role of NFAT5 in inflammatory disorders associated with osmotic stress. Curr Genomics 11: 584-590.

29 Wang G, Chen HW, Oktay Y, Zhang J, Allen EL, et al. (2010) PNPASE regulates RNA import into mitochondria. Cell 142: 456-467.

30 Misaka T, Miyashita T, Kubo Y (2002) Primary structure of a dynamin-related mouse mitochondrial GTPase and its distribution in brain, subcellular localization, and effect on mitochondrial morphology. J Biol Chem 277: 15834-15842.

31 Yu P, Huang B, Shen M, Lau C, Chan E, et al. (2001) p15(PAF), a novel PCNA associated factor with increased expression in tumor tissues. Oncogene 20: 484-489.

32 Dumond JB, Nicol MR, Kendrick RN, Garonzik SM, Patterson KB, et al.

(2012) Pharmacokinetic modelling of efavirenz, atazanavir, lamivudine and tenofovir in the female genital tract of HIV-infected pre-menopausal women. Clin Pharmacokinet 51: 809-822.

33 Lee CG, Ren J, Cheong IS, Ban KH, Ooi LL, et al. (2003) Expression of the FAT10 gene is highly upregulated in hepatocellular carcinoma and other gastrointestinal and gynecological cancers. Oncogene 22: 2592-2603.

34 Houstek J, Pickova A, Vojtiskova A, Mracek T, Pecina P, et al. (2006) Mitochondrial diseases and genetic defects of ATP synthase. Biochim Biophys Acta 1757: 1400-1405.

35 Lewis W, Day BJ, Copeland WC (2003) Mitochondrial toxicity of NRTI antiviral drugs: an integrated cellular perspective. Nat Rev Drug Discov 2: 812-822.

36 Anton PA, Cranston RD, Kashuba A, Hendrix CW, Bumpus NN, et al. (2012) RMP-02/MTN-006: A Phase 1 Rectal Safety, Acceptability, Pharmacokinetic, and Pharmacodynamic Study of Tenofovir 1% Gel Compared with Oral Tenofovir Disoproxil Fumarate. AIDS Res Hum Retroviruses 28: 1412-1421.

37 Martin M, Rehani K, Jope RS, Michalek SM (2005) Toll-like receptor-mediated cytokine production is differentially regulated by glycogen synthase kinase 3. Nat Immunol 6: 777-784.

38 Gee K, Angel JB, Ma W, Mishra S, Gajanayaka N, et al. (2006) Intracellular HIV-Tat expression induces IL-10 synthesis by the CREB-1 transcription factor through Ser133 phosphorylation and its regulation by the ERK1/2 MAPK in human monocytic cells. J Biol Chem 281: 31647-31658.

39 Konkel JE, Chen W (2011) Balancing acts: the role of TGF-beta in the mucosal immune system. Trends Mol Med 17: 668-676.

40 Surh CD, Sprent J (2012) TGF-beta puts the brakes on homeostatic proliferation. Nat Immunol 13: 628-630.

41 Ansel KM, Harris RB, Cyster JG (2002) CXCL13 is required for B1 cell homing, natural antibody production, and body cavity immunity. Immunity 16: 67-76.

42 Forster R, Davalos-Misslitz AC, Rot A (2008) CCR7 and its ligands: balancing immunity and tolerance. Nat Rev Immunol 8: 362-371.

43 Naranbhai V, Abdool Karim SS, Altfeld M, Samsunder N, Durgiah R, et al. (2012) Innate Immune Activation Enhances HIV Acquisition in Women, Diminishing the Effectiveness of Tenofovir Microbicide Gel. J Infect Dis.

44 Perazella MA (2010) Tenofovir-induced kidney disease: an acquired renal tubular mitochondriopathy. Kidney Int 78: 1060-1063.

45 Modica-Napolitano JS, Kulawiec M, Singh KK (2007) Mitochondria and human cancer. Curr Mol Med 7: 121-131.

46 Ni Chonghaile T, Sarosiek KA, Vo TT, Ryan JA, Tammareddi A, et al. (2011) Pretreatment mitochondrial priming correlates with clinical response to cytotoxic chemotherapy. Science 334: 1129-1133.

47 Shidara Y, Yamagata K, Kanamori T, Nakano K, Kwong JQ, et al. (2005) Positive contribution of pathogenic mutations in the mitochondrial genome to the promotion of cancer by prevention from apoptosis. Cancer Res 65: 1655-1663.

48 Kashuba AD, Patterson KB, Dumond JB, Cohen MS (2012) Pre-exposure prophylaxis for HIV prevention: how to predict success. Lancet 379: 2409-2411.

49 Jain M, Zhang L, Patterson EE, Kebebew E (2011) KIAA0101 is overexpressed, and promotes growth and invasion in adrenal cancer. PLoS ONE 6: e26866.

50 Ren J, Kan A, Leong SH, Ooi LL, Jeang KT, et al. (2006) FAT10 plays a role in the regulation of chromosomal stability. J Biol Chem 281: 11413-11421.

51 Ren J, Wang Y, Gao Y, Mehta SB, Lee CG (2011) FAT10 mediates the effect of TNF-alpha in inducing chromosomal instability. J Cell Sci 124: 3665-3675.

52 Ayers KM, Clive D, Tucker WE, Jr., Hajian G, de Miranda P (1996) Non-clinical toxicology studies with zidovudine: genetic toxicity tests and carcinogenicity bioassays in mice and rats. Fundam Appl Toxicol 32: 148-158.**1** Abdool Karim Q, Abdool Karim SS, Frohlich JA, Grobler AC, Baxter C, et al. (2010) Effectiveness and safety of tenofovir gel, an antiretroviral microbicide, for the prevention of HIV infection in women. Science 329: 1168-1174.

12